JCTC Journal of Chemical Theory and Computation

Article

pubs.acs.org/JCTC

Assessment of n-Electron Valence State Perturbation Theory for Vertical Excitation Energies

Igor Schapiro, Kantharuban Sivalingam, and Frank Neese*

Max Planck Institute for Chemical Energy Conversion, Stiftstr. 34-36, 45470 Mülheim an der Ruhr, Germany

ABSTRACT: The multireference n-electron Valence State Perturbation Theory is applied to a benchmark set of 28 organic molecules compiled by Schreiber et al. *J. Chem. Phys.* (2008) 128, 13. Different types of low-lying vertical excitation energies are computed using the same geometries and TZVP basis set as in the original work. The previously published coupled cluster CC3 results are used as a reference. The complete active space second order perturbation theory (CASPT2) results, as well as the results of second order N-electron valence perturbation theory (NEVPT2) (both in their single-state variants) are evaluated against this reference set, which includes 153 singlet and 72 triplet vertical transition energies. NEVPT2 calculations are carried out in two variants: the partially contracted (PC) and the strongly contracted (SC) scheme. The statistical evaluation with respect to CC3 is found to be similar for both: the mean unsigned deviations is 0.28 eV for singlets and 0.16 eV for triplets for PC-NEVPT2, while it is 0.23 and 0.17 eV for SC-NEVPT2, respectively. Further analysis has shown that deficiencies in the zeroth-order wave functions, in particular for the subset of $\pi \rightarrow \pi^*$ singlet excitations, are responsible for the largest deviations from CC3. Those states have either a charge transfer or an ionic character. For the remaining singlet and all triplet excitations the general trend was established that NEVPT2 tends to slightly overestimate excitation energies while CASPT2 slightly underestimates them. However, overall, both methods are of very similar accuracy provided that the IPEA shift is used in the CASPT2 method. Interestingly, the conclusions reached in this study are independent of the orbital canonicalization scheme used in the NEVPT2 calculation.

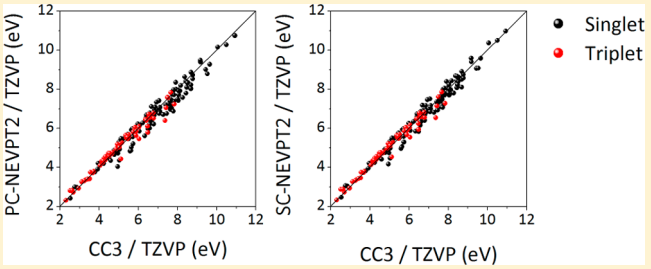

1. INTRODUCTION

In a recent study, Schreiber et al.[1] have provided a benchmark set for vertical excitation energy calculations in closed shell systems. This set consists of 225 electronically excited states of 28 medium-sized organic molecules that were benchmarked by *ab initio* methods. The vertical excitations were calculated using complete active space second order perturbation theory[2] (CASPT2) and coupled cluster methods (CC2, CCSD, and CC3). The results were compared to available highly correlated *ab initio* data from previous studies. For 104 singlet and 63 triplet excited states best theoretical estimates (TBE) were proposed. In addition, an extensive literature survey of experimental data was reported. However, due to obvious limitations in the comparison to experimental data, the benchmark set reported by Schreiber et al. was accepted as a reference for calibration of semiempirical methods[3] and development of density functionals.[4] The work by Schreiber et al. constitutes an important contribution, as it provides an excellent and carefully compiled standardized data set, against which new methods can be evaluated.[5] However, we emphasize that the validity of such an evaluation is confined to the domain of organic closed shell molecules. The conclusions reached will not be valid for systems, such as open shell transition metal complexes where the excited state electronic structures are much more complex than in organic closed shell systems. This point will be further discussed in the concluding sections of this paper.

In the present study, we investigate this set of molecules by means of n-Electron Valence State Perturbation Theory (NEVPT) developed by Angeli et al.[6] This NEVPT method is a multiconfigurational perturbation approach based on a zeroth-order description that is provided by a complete active space self-consistent field (CASSCF) wave function. In this respect, NEVPT at second order (NEVPT2) is most readily compared to the highly popular complete active space second order perturbation (CASPT2) method. However, there are a few important methodological differences between the two approaches. In particular, NEVPT2 relies on a more advanced zeroth-order Hamiltonian (the Dyall Hamiltonian[7]) that partially incorporates two body terms, while CASPT2 relies on a zeroth-order Hamiltonian that is essentially of one body nature (consisting of projected generalized Fock operators), analogous to second-order Möller–Plesset perturbation theory (MP2). However, both NEVPT2 and CASPT2 coincide with MP2 in the case of a vanishing active space. The use of the Dyall Hamiltonian at zeroth-order provides the NEVPT2 approach with two desirable properties:[6a,b,d,8] (i) size consistency (strict separability) and (ii) the absence of intruder states. The second point is more relevant in practice, as the appearance of an intruder state, results in unphysical dissociation and excitation energies. As is widely practiced,

Received: February 21, 2013

   dx.doi.org/10.1021/ct400136y | *J. Chem. Theory Comput.* XXXX, XXX, XXX–XXX

these shortcomings can be addressed by either expanding the active space[9] or using the intruder state removal shifts.[10] However, neither solution is fully satisfactory, as the former is not always feasible and requires careful usage and the latter leads to a dependence of the results on the user defined shift (which also requires some calibration to be chosen consistently). Also, it is important to note that in 2004 the so-called ionization potential−electron affinity (IPEA)[11] shift of the zeroth-order Hamiltonian was introduced to compensate for a systematic underestimation of the excitation energies of the CASPT2 method. The implementation in the present version of the Molcas quantum chemistry package[12] uses a default value of 0.25 a.u. determined from dissociation energies, spectroscopic constants, excitation energies and ionization energies for molecules and transition metal atoms.[11] This shift is known to lead to an increase of excitation energies by 0.1−0.3 eV and therefore considerably improved the CASPT2 results relative to CC3, as suggested by Schreiber et al.[1] However, more recent work on transition metal complexes induced a debate about the appropriate choice of the shift, and consequently, an increased IPEA shift was proposed.[13] In our opinion, it is one of the attractive and desirable features of the NEVPT2 approach, that once the zeroth-order wave function is defined, no further adjustments are possible and hence the second-order perturbation energy is completely defined through the zeroth-order wave function. A further, perhaps less important, difference between CASPT2 concerns the internal contraction scheme. In CASPT2, a first-order-interacting space (FOIS) construction is chosen that, in general, it leads to a nonorthogonal and potentially linearly dependent set of CSFs. Thus, in order to arrive at the second-order perturbation energy, one needs to iteratively solve a potentially ill conditioned linear equation system. While in practice this does not appear to present any problem, the procedure necessitates the storage of the first order wave function amplitudes which becomes computationally and I/O demanding for larger systems. However, NEVPT2 is available in two variants: the partially contracted (PC) and the strongly contracted (SC) NEVPT2 method. In the partially contracted version, the FOIS is spanned in the same way as in the internally contracted CASPT2. Thus, in this variant one works with a FOIS that is nonorthogonal and might be linearly dependent. Unlike in CASPT2, the solution of the linear equation system is avoided by a transformation into the energy eigenbasis of Dyall's Hamiltonian. The procedure requires the diagonalization of the active part of Dyall's Hamiltonian, the largest matrix being cubic in the number of active orbitals. In the strongly contracted version, the representation of the FOIS is more compact and more importantly the potential linear dependencies are avoided since the FOIS is spanned by a set of orthonormal CSFs. It should be noted that both variants of NEVPT2 are invariant to unitary transformation of the active orbitals. The partially contracted NEVPT2 can be formulated to become invariant to unitary transformation of the inactive and virtual orbitals.[14] All results assembled so far point to SC-NEVPT2 and PC-NEVPT2 being of similar quality.[15] The SC version might be considered more approximate due to the reduced flexibility in the FOIS; therefore, a detailed numerical comparison of the two contraction schemes seems warranted. The compactness of the FOIS in SC-NEVPT2 leads to an exceptionally efficient implementation. In particular, in combination with the resolution of the identity (RI) approximation, SC-NEVPT2 typically does not require much more time than a single closed-shell RI-MP2 calculation (for each state). In fact, the NEVPT2 step is usually much faster than the preceding solution of the CASSCF equations.

In previous work, Angeli and co-workers have already addressed several critical systems from this benchmark set, using the NEVPT approach. Among those are acetone,[16] ethene,[15d,17] formaldehyde,[16] furan,[18] all-*E*-octatetraene,[15c] pyrrole,[8,15b] and *s*-tetrazine.[15e] However, often expanded active spaces, extensive basis sets with diffuse functions, and higher order perturbation treatments were involved. Obviously, all of the above is necessary if comparison to experimental data is the focus of the investigation. However, the aim of this work is to assess NEVPT2 for vertical excitation energies under the same conditions as the original benchmark by Schreiber et al.[1] Hence, we strictly follow the active space selection, the number of states averaged over, and the basis sets used in the original publication in order to provide for a clean comparison between NEVPT2 and CASPT2 to the CC3 data reported by Schreiber et al. This data is certainly a good reference point because it was shown that CC3 has a mean absolute error of only 0.016 eV for singles dominated singlet as well as triplet excitation energies compared to Full CI results.[19]

This work is organized as follows: The details of the NEVPT2 and CASPT2 calculations are explained in section 2, Computational Details. The resulting excitation energies are compared to CC3 results from Schreiber et al.[1] in section 3, Results and Discussion. This section also includes statistical evaluations of the deviations between the different methods, grouped by the type of excitation and spin symmetry. Furthermore, we discuss the effect of the contraction scheme used in NEVPT2 as well as the orbital canonicalization. Then, we analyze the influence of the IPEA shift on CASPT2 excitation energies, and we compare a subset of the excitation energies to the recently published EOM-CCSDT-3 data.

2. COMPUTATIONAL DETAILS

The geometries optimized at the MP2/6-31G* level by Schreiber et al. and the same TZVP basis sets[20] were used for all calculations. To ensure the maximum comparability with the original calculations the CASSCF energy and orbital gradient convergence thresholds were set to 10^{-9} Hartree and 10^{-5}, respectively. Furthermore, the molecular symmetry was used. Again, in order to provide strictly comparable results, obtained with Molcas, each multiplicity and symmetry block was computed separately although ORCA has the capability to average states of different spatial and/or spin symmetry. In cases where several roots of the same symmetry were required, state-average (SA)-CASSCF was used. In all cases, the CASSCF energies were reproduced within the accuracy of the convergence. However, different symmetries were used for benzene and *s*-triazine. The original study[1] imposed C_S symmetry for both molecules while we have used the automatic reduction of symmetry in ORCA. Hence, the D_{6h} point group symmetry of benzene and D_{3h} of *s*-triazine were reduced to the Abelian subgroups D_{2h} and C_{2v}, respectively.

The SC-NEVPT2[6b,d] calculations were performed using version 2.9 of the ORCA program package into which SC-NEVPT2 has been introduced in an efficient implementation.[21] In the program default setting, the CASSCF wave function is truncated in the construction of the three- and four-body density matrices by eliminating configurations with a weight smaller than a threshold of 10^{-13}. For this benchmark, we have disabled the truncation. In order to evaluate the effect of the

dx.doi.org/10.1021/ct400136y | J. Chem. Theory Comput. XXXX, XXX, XXX−XXX

Table 1. Vertical Excitation Energies ΔE (eV) for Singlet States

			NEVPT2					
molecule	state	type	PC/1	SC/1	PC/0	SC/0	CASPT2	CC3
ethene	$1\ ^1B_{1u}$	$\pi \rightarrow \pi^*$	8.64	8.69	8.64	8.69	8.62	8.37
E-butadiene	$1\ ^1B_u$	$\pi \rightarrow \pi^*$	6.21	6.31	6.14	6.25	6.42	6.58
	$2\ ^1A_g$	$\pi \rightarrow \pi^*$	6.80	6.82	6.86	6.88	6.61	6.77
all-*E*-hexatriene	$1\ ^1B_u$	$\pi \rightarrow \pi^*$	4.84	4.96	4.84	4.96	5.35	5.58
	$2\ ^1A_g$	$\pi \rightarrow \pi^*$	5.56	5.59	5.56	5.59	5.52	5.72
all-*E*-octatetraene	$2\ ^1A_g$	$\pi \rightarrow \pi^*$	4.72	4.74	4.73	4.75	4.64	4.97
	$1\ ^1B_u$	$\pi \rightarrow \pi^*$	4.04	4.17	4.04	4.18	4.70	4.94
	$2\ ^1B_u{}^a$	$\pi \rightarrow \pi^*$	5.86	5.89	5.86	5.89	5.74	6.06
	$3\ ^1A_g{}^a$	$\pi \rightarrow \pi^*$	5.97	6.24	5.97	6.24	6.19	6.50
	$4\ ^1A_g{}^a$	$\pi \rightarrow \pi^*$	6.67	6.71	6.67	6.71	6.55	6.81
	$3\ ^1B_u{}^a$	$\pi \rightarrow \pi^*$	8.35	8.40	8.35	8.39	8.03	7.91
cyclopropene	$1\ ^1B_1$	$\sigma \rightarrow \pi^*$	6.85	6.85	6.85	6.85	6.76	6.90
	$1\ ^1B_2$	$\pi \rightarrow \pi^*$	7.07	7.18	7.07	7.14	7.06	7.10
cyclopentadiene	$1\ ^1B_2$	$\pi \rightarrow \pi^*$	5.21	5.30	5.16	5.24	5.52	5.73
	$2\ ^1A_1$	$\pi \rightarrow \pi^*$	6.72	6.74	6.78	6.81	6.48	6.61
	$3\ ^1A_1$	$\pi \rightarrow \pi^*$	8.22	8.51	8.27	8.56	8.39	8.69
norbornadiene	$1\ ^1A_2$	$\pi \rightarrow \pi^*$	5.04	5.07	5.02	5.05	5.37	5.64
	$1\ ^1B_2$	$\pi \rightarrow \pi^*$	5.79	5.84	5.77	5.81	6.12	6.49
	$2\ ^1B_2$	$\pi \rightarrow \pi^*$	6.97	7.10	7.00	7.13	7.31	7.64
	$2\ ^1A_2$	$\pi \rightarrow \pi^*$	7.03	7.07	7.07	7.10	7.42	7.71
benzene	$1\ ^1B_{2u}$	$\pi \rightarrow \pi^*$	5.21	5.24	5.21	5.24	5.04	5.07
	$1\ ^1B_{1u}$	$\pi \rightarrow \pi^*$	6.40	6.47	6.40	6.47	6.43	6.68
	$1\ ^1E_{1u}$	$\pi \rightarrow \pi^*$	7.11	7.28	7.11	7.28	7.09	7.45
	$2\ ^1E_{2g}$	$\pi \rightarrow \pi^*$	8.42	8.45	8.42	8.45	8.19	8.43
naphthalene	$1\ ^1B_{3u}$	$\pi \rightarrow \pi^*$	4.37	4.39	4.38	4.40	4.24	4.27
	$1\ ^1B_{2u}$	$\pi \rightarrow \pi^*$	4.37	4.47	4.36	4.47	4.80	5.03
	$2\ ^1A_g$	$\pi \rightarrow \pi^*$	6.23	6.27	6.22	6.26	5.87	5.98
	$1\ ^1B_{1g}$	$\pi \rightarrow \pi^*$	6.15	6.20	6.15	6.20	6.02	6.07
	$2\ ^1B_{3u}$	$\pi \rightarrow \pi^*$	5.61	5.85	5.61	5.85	6.12	6.33
	$2\ ^1B_{1g}$	$\pi \rightarrow \pi^*$	6.22	6.41	6.22	6.41	6.47	6.79
	$2\ ^1B_{2u}$	$\pi \rightarrow \pi^*$	6.01	6.17	6.02	6.17	6.36	6.57
	$3\ ^1A_g$	$\pi \rightarrow \pi^*$	6.85	6.90	6.84	6.89	6.67	6.90
	$3\ ^1B_{2u}$	$\pi \rightarrow \pi^*$	7.81	8.09	7.82	8.10	8.11	8.44
	$3\ ^1B_{3u}$	$\pi \rightarrow \pi^*$	7.92	7.98	7.92	7.98	7.71	8.12
furan	$1\ ^1B_2$	$\pi \rightarrow \pi^*$	6.42	6.59	6.36	6.52	6.52	6.60
	$2\ ^1A_1$	$\pi \rightarrow \pi^*$	6.75	6.79	6.80	6.83	6.52	6.62
	$3\ ^1A_1$	$\pi \rightarrow \pi^*$	8.35	8.62	8.44	8.72	8.32	8.53
pyrrole	$2\ ^1A_1$	$\pi \rightarrow \pi^*$	6.56	6.60	6.58	6.63	6.30	6.40
	$1\ ^1B_2$	$\pi \rightarrow \pi^*$	6.78	6.90	6.74	6.87	6.33	6.71
	$3\ ^1A_1$	$\pi \rightarrow \pi^*$	8.19	8.44	8.22	8.47	8.06	8.17
imidazole	$1\ ^1A''$	$n \rightarrow \pi^*$	6.97	7.00	6.94	6.97	6.81	6.82
	$2\ ^1A'$	$\pi \rightarrow \pi^*$	6.80	6.85	6.83	6.89	6.58	6.58
	$3\ ^1A'$	$\pi \rightarrow \pi^*$	6.85	6.99	6.90	7.04	6.71	7.10
	$2\ ^1A''$	$n \rightarrow \pi^*$	8.01	8.06	8.02	8.07	7.90	7.93
	$4\ ^1A'$	$\pi \rightarrow \pi^*$	8.39	8.68	8.45	8.73	8.14	8.45
pyridine	$1\ ^1B_2$	$\pi \rightarrow \pi^*$	5.33	5.36	5.33	5.35	5.08	5.15
	$1\ ^1B_1$	$n \rightarrow \pi^*$	5.26	5.28	5.26	5.28	5.17	5.05
	$1\ ^1A_2$	$n \rightarrow \pi^*$	5.46	5.50	5.46	5.50	5.51	5.50
	$2\ ^1A_1$	$\pi \rightarrow \pi^*$	7.09	7.17	7.08	7.17	7.10	6.85
	$3\ ^1A_1$	$\pi \rightarrow \pi^*$	7.23	7.50	7.23	7.50	7.44	7.70
	$2\ ^1B_2$	$\pi \rightarrow \pi^*$	7.10	7.38	7.11	7.38	7.28	7.59
	$4\ ^1A_1$	$\pi \rightarrow \pi^*$	8.03	8.11	8.07	8.15	7.95	8.68
	$3\ ^1B_2$	$\pi \rightarrow \pi^*$	8.53	8.58	8.53	8.58	8.66	8.77
pyrazine	$1\ ^1B_{3u}$	$n \rightarrow \pi^*$	4.20	4.25	4.20	4.25	4.12	4.24
	$1\ ^1A_u$	$n \rightarrow \pi^*$	4.93	4.99	4.95	5.01	4.90	5.05
	$1\ ^1B_{2u}$	$\pi \rightarrow \pi^*$	5.31	5.34	5.30	5.33	5.00	5.02
	$1\ ^1B_{2g}$	$n \rightarrow \pi^*$	5.86	5.91	5.86	5.91	5.68	5.74
	$1\ ^1B_{1g}$	$n \rightarrow \pi^*$	6.77	6.83	6.79	6.84	6.63	6.75
	$1\ ^1B_{1u}$	$\pi \rightarrow \pi^*$	6.76	6.85	6.76	6.85	6.90	7.07

dx.doi.org/10.1021/ct400136y | J. Chem. Theory Comput. XXXX, XXX, XXX−XXX

Table 1. continued

molecule	state	type	NEVPT2 PC/1	NEVPT2 SC/1	NEVPT2 PC/0	NEVPT2 SC/0	CASPT2	CC3
	$2\ ^1B_{1u}$	$\pi \rightarrow \pi^*$	7.72	8.01	7.72	8.00	7.79	8.06
	$2\ ^1B_{2u}$	$\pi \rightarrow \pi^*$	7.43	7.69	7.44	7.70	7.51	8.05
	$1\ ^1B_{3g}$	$\pi \rightarrow \pi^*$	8.73	8.76	8.73	8.76	8.47	8.77
	$2\ ^1A_g$	$\pi \rightarrow \pi^*$	8.87	8.92	8.86	8.91	8.60	8.69
pyrimidine	$1\ ^1B_1$	$n \rightarrow \pi^*$	4.52	4.57	4.52	4.57	4.44	4.50
	$1\ ^1A_2$	$n \rightarrow \pi^*$	4.81	4.87	4.81	4.87	4.80	4.93
	$1\ ^1B_2$	$\pi \rightarrow \pi^*$	5.61	5.63	5.61	5.63	5.30	5.36
	$2\ ^1A_1$	$\pi \rightarrow \pi^*$	7.42	7.51	7.41	7.50	7.38	7.06
	$2\ ^1B_2$	$\pi \rightarrow \pi^*$	7.51	7.80	7.50	7.80	7.61	8.01
	$3\ ^1A_1$	$\pi \rightarrow \pi^*$	7.73	8.00	7.73	8.00	7.69	7.74
pyridazine	$1\ ^1B_1$	$n \rightarrow \pi^*$	3.92	3.96	3.91	3.95	3.80	3.92
	$1\ ^1A_2$	$n \rightarrow \pi^*$	4.57	4.61	4.58	4.62	4.41	4.49
	$2\ ^1A_1$	$\pi \rightarrow \pi^*$	5.46	5.48	5.47	5.49	5.17	5.22
	$2\ ^1A_2$	$n \rightarrow \pi^*$	5.89	5.95	5.89	5.95	5.67	5.74
	$2\ ^1B_1$	$n \rightarrow \pi^*$	6.68	6.74	6.69	6.75	6.49	6.41
	$1\ ^1B_2$	$\pi \rightarrow \pi^*$	7.34	7.47	7.35	7.47	7.34	6.93
	$2\ ^1B_2$	$\pi \rightarrow \pi^*$	7.25	7.50	7.25	7.51	7.35	7.55
	$3\ ^1A_1$	$\pi \rightarrow \pi^*$	7.38	7.70	7.37	7.69	7.61	7.82
s-triazine	$1\ ^1A_1''$	$n \rightarrow \pi^*$	4.65	4.77	4.65	4.76	4.68	4.78
	$1\ ^1A_2''$	$n \rightarrow \pi^*$	4.88	4.94	4.88	4.94	4.73	4.76
	$1\ ^1E''$	$n \rightarrow \pi^*$	4.87	4.94	4.87	4.95	4.74	4.81
	$1\ ^1A_2'$	$\pi \rightarrow \pi^*$	5.92	5.94	5.92	5.94	5.67	5.71
	$2\ ^1A_1'$	$\pi \rightarrow \pi^*$	7.21	7.36	7.19	7.34	7.03	7.41
	$2\ ^1E''$	$n \rightarrow \pi^*$	7.98	8.06	7.97	8.06	7.68	7.80
	$1\ ^1E'$	$\pi \rightarrow \pi^*$	7.94	8.25	7.95	8.25	7.80	8.04
	$2\ ^1E'$	$\pi \rightarrow \pi^*$	9.01	9.08	9.03	9.10	8.84	9.44
s-tetrazine	$1\ ^1B_{3u}$	$n \rightarrow \pi^*$	2.41	2.47	2.41	2.47	2.30	2.53
	$1\ ^1A_u$	$\pi \rightarrow \pi^*$	3.76	3.82	3.79	3.85	3.59	3.79
	$1\ ^1B_{1g}$	$n \rightarrow \pi^*$	5.17	5.22	5.16	5.21	4.93	4.97
	$1\ ^1B_{2u}$	$\pi \rightarrow \pi^*$	5.47	5.50	5.49	5.52	5.14	5.12
	$1\ ^1B_{2g}$	$n \rightarrow \pi^*$	5.53	5.57	5.53	5.57	5.22	5.34
	$1\ ^1B_{3g}$	$n,n \rightarrow \pi^*,\pi^*$	6.30	6.35	6.30	6.35	5.99	
	$2\ ^1A_u$	$\pi \rightarrow \pi^*$	5.70	5.77	5.68	5.75	5.44	5.46
	$2\ ^1B_{2g}$	$n \rightarrow \pi^*$	6.28	6.35	6.29	6.36	6.04	6.23
	$2\ ^1B_{1g}$	$n \rightarrow \pi^*$	6.83	6.89	6.82	6.88	6.57	6.87
	$3\ ^1B_{1g}$	$n \rightarrow \pi^*$	7.02	7.09	7.04	7.10	6.77	7.08
	$2\ ^1B_{3u}$	$n \rightarrow \pi^*$	7.11	7.18	7.12	7.19	6.76	6.67
	$1\ ^1B_{1u}$	$\pi \rightarrow \pi^*$	6.76	6.93	6.78	6.95	7.19	7.45
	$2\ ^1B_{1u}$	$\pi \rightarrow \pi^*$	6.87	7.24	6.86	7.23	7.20	7.79
	$2\ ^1B_{2u}$	$\pi \rightarrow \pi^*$	8.33	8.40	8.30	8.37	7.94	8.51
	$2\ ^1B_{3g}$	$\pi \rightarrow \pi^*$	8.10	8.24	8.08	8.22	8.32	8.47
formaladehyde	$1\ ^1A_2$	$n \rightarrow \pi^*$	4.22	4.22	4.22	4.22	3.99	3.95
	$1\ ^1B_1$	$\sigma \rightarrow \pi^*$	9.40	9.40	9.40	9.40	9.14	9.18
	$2\ ^1A_1$	$\pi \rightarrow \pi^*$	8.79	9.08	8.66	8.96	9.19	9.53
acetone	$1\ ^1A_2$	$n \rightarrow \pi^*$	4.47	4.49	4.47	4.49	4.44	4.40
	$1\ ^1B_1$	$\sigma \rightarrow \pi^*$	9.50	9.59	9.50	9.59	9.27	9.17
	$2\ ^1A_1$	$\pi \rightarrow \pi^*$	9.28	9.58	9.22	9.55	9.21	9.65
p-benzoquinone	$1\ ^1A_u$	$n \rightarrow \pi^*$	2.99	3.04	2.99	3.05	2.78	2.85
	$1\ ^1B_{1g}$	$n \rightarrow \pi^*$	3.00	3.06	3.00	3.06	2.76	2.75
	$1\ ^1B_{3g}$	$\pi \rightarrow \pi^*$	4.35	4.43	4.27	4.35	4.61	4.59
	$1\ ^1B_{1u}$	$\pi \rightarrow \pi^*$	4.85	5.02	4.82	4.99	5.31	5.62
	$1\ ^1B_{3u}$	$n \rightarrow \pi^*$	5.88	5.96	5.87	5.95	5.64	5.82
	$2\ ^1B_{3g}$	$\pi \rightarrow \pi^*$	6.70	6.82	6.78	6.90	6.92	7.27
	$2\ ^1B_{1u}$	$\pi \rightarrow \pi^*$	7.72	7.78	7.73	7.79	7.91	7.82
formamide	$1\ ^1A''$	$n \rightarrow \pi^*$	5.93	5.93	5.93	5.93	5.63	5.65
	$2\ ^1A'$	$\pi \rightarrow \pi^*$	7.58	7.81	7.62	7.84	7.43	8.27
	$3\ ^1A'$	$\pi \rightarrow \pi^*$	10.75	10.97	10.84	11.05	10.48	10.93
acetamide	$1\ ^1A''$	$n \rightarrow \pi^*$	5.97	5.96	5.97	5.96	5.80	5.69
	$2\ ^1A'$	$\pi \rightarrow \pi^*$	7.48	7.69	7.48	7.68	7.30	7.67

dx.doi.org/10.1021/ct400136y | J. Chem. Theory Comput. XXXX, XXX, XXX−XXX

Table 1. continued

molecule	state	type	NEVPT2 PC/1	NEVPT2 SC/1	NEVPT2 PC/0	NEVPT2 SC/0	CASPT2	CC3
	$3\ ^1A'$	$\pi \rightarrow \pi^*$	10.28	10.50	10.31	10.52	10.04	10.50
propanamide	$1\ ^1A''$	$n \rightarrow \pi^*$	5.99	5.99	5.99	5.98	5.72	5.72
	$2\ ^1A'$	$\pi \rightarrow \pi^*$	7.40	7.61	7.41	7.60	7.23	7.62
	$3\ ^1A'$	$\pi \rightarrow \pi^*$	10.16	10.37	10.16	10.38	9.89	10.06
cytosine	$2\ ^1A'$	$\pi \rightarrow \pi^*$	4.70	4.78	4.77	4.85	4.58	
	$1\ ^1A''$	$n \rightarrow \pi^*$	5.50	5.56	5.50	5.56	5.20	
	$2\ ^1A''$	$n \rightarrow \pi^*$	5.73	5.80	5.73	5.79	5.45	
	$3\ ^1A'$	$\pi \rightarrow \pi^*$	5.65	5.74	5.70	5.79	5.58	
	$4\ ^1A'$	$\pi \rightarrow \pi^*$	6.47	6.70	6.48	6.70	6.37	
	$5\ ^1A'$	$\pi \rightarrow \pi^*$	6.83	6.98	6.80	6.95	6.79	
	$6\ ^1A'$	$\pi \rightarrow \pi^*$	8.06	8.21	8.11	8.25	7.85	
thymine	$1\ ^1A''$	$n \rightarrow \pi^*$	4.96	5.04	4.94	5.02	4.97	
	$2\ ^1A'$	$\pi \rightarrow \pi^*$	5.05	5.18	5.05	5.18	5.07	
	$3\ ^1A'$	$\pi \rightarrow \pi^*$	6.32	6.43	6.43	6.54	6.27	
	$2\ ^1A''$	$n \rightarrow \pi^*$	6.49	6.57	6.46	6.54	6.43	
	$4\ ^1A'$	$\pi \rightarrow \pi^*$	6.44	6.64	6.34	6.54	6.50	
	$3\ ^1A''$	$n \rightarrow \pi^*$	6.69	6.89	6.62	6.83	6.91	
	$4\ ^1A''$	$n \rightarrow \pi^*$	7.41	7.56	7.39	7.54	7.30	
	$5\ ^1A'$	$\pi \rightarrow \pi^*$	7.35	7.62	7.36	7.64	7.30	
uracil	$1\ ^1A''$	$n \rightarrow \pi^*$	4.92	4.99	4.89	4.97	4.93	
	$2\ ^1A'$	$\pi \rightarrow \pi^*$	5.27	5.39	5.29	5.40	5.23	
	$3\ ^1A'$	$\pi \rightarrow \pi^*$	6.22	6.33	6.31	6.43	6.17	
	$2\ ^1A''$	$n \rightarrow \pi^*$	6.42	6.49	6.39	6.47	6.37	
	$3\ ^1A''$	$n \rightarrow \pi^*$	6.70	6.89	6.62	6.83	7.22	
	$4\ ^1A'$	$\pi \rightarrow \pi^*$	6.68	6.86	6.61	6.79	6.69	
	$4\ ^1A''$	$n \rightarrow \pi^*$	7.27	7.42	7.24	7.40	6.94	
	$5\ ^1A'$	$\pi \rightarrow \pi^*$	7.38	7.64	7.40	7.66	7.33	
adenine	$2\ ^1A'$	$\pi \rightarrow \pi^*$	5.07	5.22	5.07	5.21	5.18	
	$3\ ^1A'$	$\pi \rightarrow \pi^*$	5.43	5.46	5.43	5.47	5.20	
	$1\ ^1A''$	$n \rightarrow \pi^*$	5.36	5.43	5.36	5.44	5.38	
	$2\ ^1A''$	$n \rightarrow \pi^*$	6.07	6.16	6.07	6.16	6.10	
	$4\ ^1A'$	$\pi \rightarrow \pi^*$	6.45	6.68	6.45	6.65	6.59	
	$5\ ^1A'$	$\pi \rightarrow \pi^*$	6.82	6.95	6.82	6.96	6.58	
	$6\ ^1A'$	$\pi \rightarrow \pi^*$	6.95	7.01	6.95	7.03	6.40	
	$7\ ^1A'$	$\pi \rightarrow \pi^*$	7.72	7.83	7.72	7.85	7.42	

[a]These states of the all-*E*-octatetraene were not listed in the table of the original work although included in the statistical evaluation.

contraction scheme, we have also carried out PC-NEVPT2 calculations using the implementation in Molpro[22] quantum chemistry package.

We have also studied the importance of the orbital canonicalization. In the accurate scheme the orbital energies for the doubly occupied and virtual orbitals that appear in the Dyall Hamiltonian[7] (used for the definition of the zeroth-order Hamiltonian in NEVPT2) are obtained through the diagonalization of the state-specific Fock operator ("nev_canonstep 1" option in ORCA). Since this requires a separate set of orbitals for each state one can certainly save significant computer time by taking the diagonal elements instead to use the state-averaged (canonicalized) orbitals. This setup corresponds to the option "nev_canonstep 0" in ORCA; therefore, the resulting energies are labeled as PC/0-NEVPT2 and SC/0-NEVPT2 in the following to distinguish them from the more accurate state-specific calculations identified as PC/1-NEVPT2 and SC/1-NEVPT2. If no label is given for the NEVPT2 energies then it refers to the latter scheme, namely the state-specific orbitals and energies. The major fraction of the calculations in this benchmark involves the state-averaged CASSCF procedure; hence, we assess the effect of the orbital canonicalization scheme to estimate its effect. The results of the PC/0- and SC/0-NEVPT2 calculations are discussed in the section 3.5. It should be carefully noted that the term "state specific" is not used in the sense that the orbitals for each state are optimal (there has been no state specific orbital optimization) but rather that the orbitals for each state are different because they diagonalize state specific Fock operators.

The benchmark set includes qualitatively different excitations: $\pi \rightarrow \pi^*$, $n \rightarrow \pi^*$, and $\sigma \rightarrow \pi^*$, but no Rydberg states are included in the data set due to the limitation of the basis set imposed by the CC3 method. Hence, neither pure nor mixed Rydberg states are part of the benchmark set. However, the low lying Rydberg states are mixing with valence excited states, which are known to be exaggerated at the single state (SS) CASPT2 level. Therefore, multistate (MS) CASPT2[23] was employed in the original benchmark whenever more than one root is computed for each symmetry. Due to missing implementation of the quasi-degenerate (QD) NEVPT2[24] in ORCA and Molpro, only state-specific NEVPT2 calculations were performed. In order to compare the NEVPT2 calculations on the same basis, we have repeated all calculations with Molcas 7.6 program[12a] to obtain the SS-CASPT2 energies,

dx.doi.org/10.1021/ct400136y | J. Chem. Theory Comput. XXXX, XXX, XXX−XXX

Table 2. Vertical Excitation Energies ΔE (eV) for Triplets States

			NEVPT2					
molecule	state	type	PC/1	SC/1	PC/0	SC/0	CASPT2	CC3
ethene	$1\ ^3B_{1u}$	$\pi \rightarrow \pi^*$	4.60	4.60	4.60	4.60	4.60	4.48
E-butadiene	$1\ ^3B_u$	$\pi \rightarrow \pi^*$	3.38	3.39	3.38	3.39	3.34	3.32
	$1\ ^3A_g$	$\pi \rightarrow \pi^*$	5.27	5.28	5.27	5.28	5.16	5.17
all-*E*-hexatriene	$1\ ^3B_u$	$\pi \rightarrow \pi^*$	2.73	2.74	2.73	2.74	2.71	2.69
	$1\ ^3A_g$	$\pi \rightarrow \pi^*$	4.39	4.40	4.39	4.40	4.31	4.32
all-*E*-octatetraene	$1\ ^3B_u$	$\pi \rightarrow \pi^*$	2.32	2.33	2.32	2.33	2.33	2.30
	$1\ ^3A_g$	$\pi \rightarrow \pi^*$	3.72	3.73	3.72	3.73	3.70	3.67
cyclopropene	$1\ ^3B_2$	$\pi \rightarrow \pi^*$	4.54	4.56	4.54	4.54	4.35	4.34
	$1\ ^3B_1$	$\sigma \rightarrow \pi^*$	6.58	6.58	6.58	6.58	6.51	6.62
cyclopentadiene	$1\ ^3B_2$	$\pi \rightarrow \pi^*$	3.32	3.33	3.32	3.33	3.28	3.25
	$1\ ^3A_1$	$\pi \rightarrow \pi^*$	5.22	5.23	5.22	5.23	5.10	5.09
norbornadiene	$1\ ^3A_2$	$\pi \rightarrow \pi^*$	3.79	3.81	3.80	3.81	3.75	3.72
	$1\ ^3B_2$	$\pi \rightarrow \pi^*$	4.30	4.31	4.30	4.31	4.22	4.16
benzene	$1\ ^3B_{1u}$	$\pi \rightarrow \pi^*$	4.32	4.33	4.32	4.33	4.17	4.12
	$1\ ^3E_{1u}$	$\pi \rightarrow \pi^*$	4.98	5.00	4.98	5.00	4.89	4.90
	$1\ ^3B_{2u}$	$\pi \rightarrow \pi^*$	5.47	5.54	5.47	5.54	5.77	6.04
	$1\ ^3E_{2g}$	$\pi \rightarrow \pi^*$	7.59	7.61	7.59	7.61	7.38	7.49
naphthalene	$1\ ^3B_{2u}$	$\pi \rightarrow \pi^*$	3.26	3.28	3.26	3.27	3.18	3.11
	$1\ ^3B_{3u}$	$\pi \rightarrow \pi^*$	4.24	4.27	4.24	4.26	4.25	4.18
	$1\ ^3B_{1g}$	$\pi \rightarrow \pi^*$	4.57	4.59	4.57	4.59	4.52	4.47
	$2\ ^3B_{2u}$	$\pi \rightarrow \pi^*$	4.70	4.73	4.70	4.73	4.66	4.64
	$2\ ^3B_{3u}$	$\pi \rightarrow \pi^*$	4.44	4.53	4.44	4.54	4.97	5.11
	$1\ ^3A_g$	$\pi \rightarrow \pi^*$	5.59	5.62	5.58	5.61	5.53	5.52
	$2\ ^3B_{1g}$	$\pi \rightarrow \pi^*$	5.80	5.95	5.81	5.96	6.22	6.48
	$2\ ^3A_g$	$\pi \rightarrow \pi^*$	6.11	6.25	6.12	6.26	6.40	6.47
	$3\ ^3A_g$	$\pi \rightarrow \pi^*$	6.52	6.56	6.52	6.56	6.57	6.79
	$3\ ^3B_{1g}$	$\pi \rightarrow \pi^*$	6.79	6.83	6.78	6.82	6.63	6.76
furan	$1\ ^3B_2$	$\pi \rightarrow \pi^*$	4.33	4.36	4.33	4.36	4.17	4.17
	$1\ ^3A_1$	$\pi \rightarrow \pi^*$	5.62	5.67	5.62	5.67	5.49	5.48
pyrrole	$1\ ^3B_2$	$\pi \rightarrow \pi^*$	4.73	4.74	4.73	4.74	4.52	4.48
	$1\ ^3A_1$	$\pi \rightarrow \pi^*$	5.68	5.70	5.68	5.70	5.53	5.51
imidazole	$1\ ^3A'$	$\pi \rightarrow \pi^*$	4.77	4.80	4.73	4.77	4.67	4.69
	$2\ ^3A'$	$\pi \rightarrow \pi^*$	5.89	5.93	5.87	5.90	5.77	5.79
	$1\ ^3A''$	$n \rightarrow \pi^*$	6.46	6.49	6.43	6.46	6.36	6.37
	$3\ ^3A'$	$\pi \rightarrow \pi^*$	6.61	6.67	6.59	6.66	6.64	6.55
	$4\ ^3A'$	$\pi \rightarrow \pi^*$	7.06	7.15	7.08	7.17	7.18	7.42
	$2\ ^3A''$	$n \rightarrow \pi^*$	7.57	7.61	7.58	7.62	7.51	7.51
pyridine	$1\ ^3A_1$	$\pi \rightarrow \pi^*$	4.47	4.48	4.47	4.48	4.28	4.25
	$1\ ^3B_1$	$n \rightarrow \pi^*$	4.58	4.60	4.58	4.60	4.55	4.50
	$1\ ^3B_2$	$\pi \rightarrow \pi^*$	4.94	4.97	4.93	4.96	4.88	4.86
	$2\ ^3A_1$	$\pi \rightarrow \pi^*$	5.13	5.16	5.13	5.16	5.02	5.05
	$1\ ^3A_2$	$n \rightarrow \pi^*$	5.46	5.49	5.46	5.49	5.48	5.46
	$2\ ^3B_2$	$\pi \rightarrow \pi^*$	6.41	6.49	6.43	6.51	6.62	6.40
	$3\ ^3B_2$	$\pi \rightarrow \pi^*$	7.23	7.28	7.22	7.27	7.11	7.83
	$3\ ^3A_1$	$\pi \rightarrow \pi^*$	7.83	7.87	7.83	7.86	7.55	7.66
s-tetrazine	$1\ ^3B_{3u}$	$n \rightarrow \pi^*$	1.64	1.69	1.63	1.68	1.62	1.89
	$1\ ^3A_u$	$n \rightarrow \pi^*$	3.42	3.46	3.44	3.48	3.34	3.52
	$1\ ^3B_{1g}$	$n \rightarrow \pi^*$	4.33	4.37	4.34	4.38	4.14	4.21
	$1\ ^3B_{1u}$	$\pi \rightarrow \pi^*$	4.55	4.56	4.55	4.55	4.37	4.33
	$1\ ^3B_{2u}$	$\pi \rightarrow \pi^*$	4.72	4.76	4.73	4.77	4.64	4.54
	$1\ ^3B_{2g}$	$n \rightarrow \pi^*$	5.19	5.22	5.19	5.22	4.96	4.93
	$2\ ^3A_u$	$n \rightarrow \pi^*$	5.03	5.11	5.01	5.09	4.99	5.03
	$1\ ^3B_{3g}$	$n,n \rightarrow \pi^*,\pi^*$	7.81	5.64	5.60	5.60	5.57	
	$2\ ^3B_{1u}$	$\pi \rightarrow \pi^*$	5.51	5.54	5.51	5.54	5.40	5.38
	$2\ ^3B_{2g}$	$n \rightarrow \pi^*$	6.11	6.18	6.11	6.18	5.95	6.04
	$2\ ^3B_{1g}$	$n \rightarrow \pi^*$	6.55	6.62	6.55	6.62	6.37	6.60
	$2\ ^3B_{3u}$	$n \rightarrow \pi^*$	6.72	6.78	6.73	6.79	6.53	6.53
	$2\ ^3B_{2u}$	$\pi \rightarrow \pi^*$	6.40	6.54	6.43	6.58	6.83	7.36
formaladehyde	$1\ ^3A_2$	$n \rightarrow \pi^*$	3.75	3.75	3.75	3.75	3.58	3.55

dx.doi.org/10.1021/ct400136y | J. Chem. Theory Comput. XXXX, XXX, XXX−XXX

Table 2. continued

molecule	state	type	NEVPT2 PC/1	NEVPT2 SC/1	NEVPT2 PC/0	NEVPT2 SC/0	CASPT2	CC3
	$1\,^3A_1$	$\pi \rightarrow \pi^*$	6.06	6.05	6.06	6.05	5.84	5.83
acetone	$1\,^3A_2$	$n \rightarrow \pi^*$	4.10	4.13	4.10	4.13	4.10	4.05
	$1\,^3A_1$	$\pi \rightarrow \pi^*$	6.06	6.04	6.06	6.04	6.04	6.03
p-benzoquinone	$1\,^3B_{1g}$	$n \rightarrow \pi^*$	2.82	2.88	2.82	2.88	2.62	2.51
	$1\,^3A_u$	$n \rightarrow \pi^*$	2.82	2.89	2.83	2.89	2.66	2.62
	$1\,^3B_{1u}$	$\pi \rightarrow \pi^*$	2.93	2.94	2.92	2.94	2.99	2.96
	$1\,^3B_{3g}$	$\pi \rightarrow \pi^*$	3.40	3.43	3.39	3.42	3.45	3.41
formamide	$1\,^3A''$	$n \rightarrow \pi^*$	5.64	5.65	5.54	5.54	5.42	5.36
	$1\,^3A'$	$\pi \rightarrow \pi^*$	5.81	5.87	5.78	5.85	5.61	5.74
acetamide	$1\,^3A''$	$n \rightarrow \pi^*$	5.52	5.54	5.50	5.51	5.56	5.42
	$1\,^3A'$	$\pi \rightarrow \pi^*$	5.63	5.67	5.69	5.70	5.76	5.88
propanamide	$1\,^3A''$	$n \rightarrow \pi^*$	5.54	5.60	5.54	5.54	5.48	5.45
	$1\,^3A'$	$\pi \rightarrow \pi^*$	5.86	5.90	5.73	5.81	5.74	5.90

Table 3. Statistical Analysis of the Singlet Excitation Energies with Respect to the CC3 Results[a]

	PC-NEVPT2	SC-NEVPT2	CASPT2
count	121 (47)	121 (47)	121 (47)
MSD	−0.12 eV (−0.25 eV)	−0.01 eV (−0.11 eV)	−0.17 eV (−0.17 eV)
MUD	0.28 eV (0.40 eV)	0.23 eV (0.31 eV)	0.21 eV (0.24 eV)
SD[b]	0.33 eV (0.39 eV)	0.29 eV (0.35 eV)	0.26 eV (0.27 eV)
max.	−0.92 eV (−0.92 eV)	−0.77 eV (−0.77 eV)	−0.84 eV (−0.59 eV)

[a]Analysis of a subset of CC3 excited states with a single excitation weight exceeding 90% is given in the brackets. [b]SD = standard deviation.

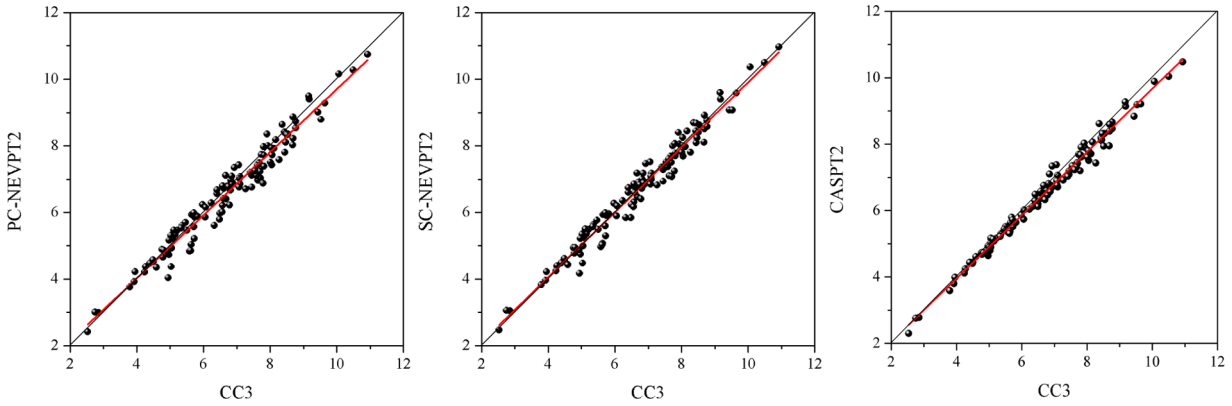

Figure 1. Correlation plots for all calculated singlet excited states. The energy is given in eV.

since they were not provided by Schreiber et al.[1] The computational details such as the number of roots in the state-average procedure and level shifts were taken from the Supporting Information provided by Schreiber et al.[1] In the following, SS-CASPT2 is simply denoted as CASPT2. In addition, we have repeated the calculations with the IPEA shift set to zero as in the original formulation of CASPT2. These results are labeled as CASPT2/IPEA0, and their discussion can be found in section 3.6.

3. RESULTS AND DISCUSSION

In this section, we present the NEVPT2 and CASPT2 results for the 153 singlet and 72 triplet valence excited states, given in Tables 1 and 2, respectively, together with CC3 results from the original study.[1] The calculated PC- and SC-NEVPT2 excitation energies are compared individually to the CC3 results. However, also, the deviation of CASPT2 from CC3 is given in order to evaluate general trends and the deviations between these methods. First we give an overview of the number and types of excited states included in this work. Then, we analyze singlet excitations by evaluating subsets of different excitation types. Next, we provide a statistical evaluation of all triplet excitations together, since their number is too small to be analyzed for different excitations separately. The effect of the contraction scheme employed in NEVPT2, and the effect of different orbital canonicalization schemes are discussed in separate sections. We also investigate the influence of the IPEA shift on the CASPT2 excitation energies by setting it to zero and obtaining the original formulation of the zeroth-order Hamiltonian. Finally, we assess a set of different reference energies computed at the EOM-CCSDT-3 level of theory.

3.1. Benchmark Set. It should be noted that there are two more states than reported in the original work. Because of the singlet and triplet B_{3g} state of *s*-tetrazine, we count 153 singlet and 72 triplet states, instead of the reported 152 and 71 states, respectively, giving a total of 225 states, instead of 223. These two states had a significant double excitation character, and therefore, their energies were only accessible at CASPT2 level

dx.doi.org/10.1021/ct400136y | J. Chem. Theory Comput. XXXX, XXX, XXX−XXX

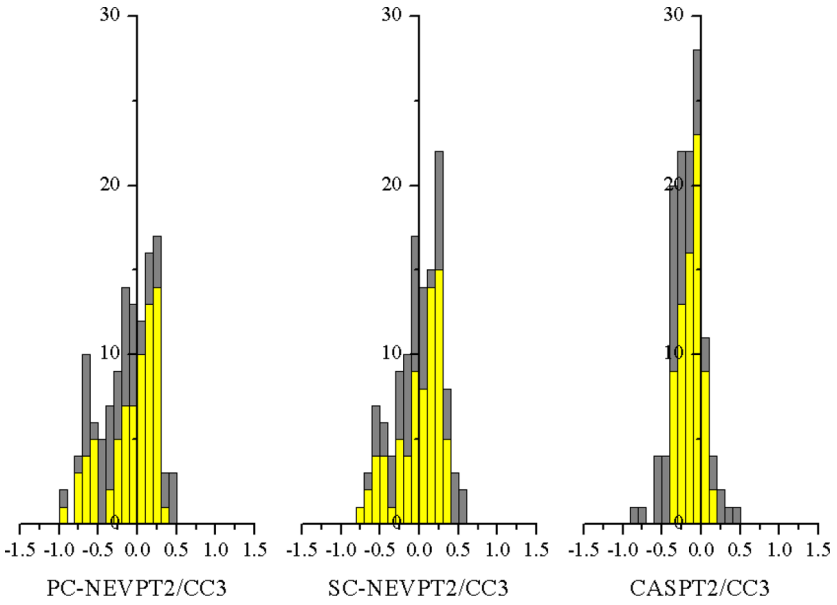

Figure 2. Histogram of the frequency of deviations in the singlet excitation energies in eV. Statistics of all excitation energies are shown in gray and those below 7 eV are represented by yellow bars.

in the original benchmark. Hence, these states are missing in the comparison to coupled cluster excitation energies as well as 31 singlet states for the four nucleobases: adenine, cytosine, thymine, and uracil, due to the size of these molecules.

3.2. Singlet Excited States. Table 3 shows the statistical evaluation of the singlet excited states. The mean signed deviations (MSD) of PC and SC-NEVPT2 compared to CC3 are −0.12 eV and −0.01 eV, respectively, while the deviation of CASPT2 from CC3 is slightly larger: −0.17 eV. The mean unsigned deviation (MUD) of 0.28 and 0.23 eV for PC- and SC-NEVPT2 is close to 0.21 eV for the CASPT2/CC3 comparison. Hence, the initial conclusion is that NEVPT2 provides very balanced results of comparable accuracy to CASPT2. The standard deviation confirms that NEVPT2 energies (0.33 eV for PC and 0.29 eV for SC) are similarly scattered as the CASPT2 results (0.26 eV). The very slight advantage of CASPT2 is also visible in the correlation plots in Figure 1 that are marginally broader for PC- and SC-NEVPT2. Surprisingly, the SC-NEVPT2 is slightly better than the formally more accurate PC variant.

Upon elimination of CC3 results with a single excitation weight of less than 90%, the MSD for NEVPT2 becomes −0.25 eV (PC) and −0.11 eV (SC), but for CASPT2, it remains −0.17 eV, as summarized in Table 3. The remaining states are clearly dominated by single excitations; therefore, they are expected to be more accurate at the CC3 level. The deviations increase for NEVPT2 compared to the full set of singlet states because the total number of excitation energies is reduced from 121 to 47, but the maximum deviation for NEVPT2/CC3 (−0.92 eV 2 $^1B_{1u}$ state of *s*-tetrazine for PC-NEVPT2 and −0.77 eV 1 ^1B_u state of octatetraene for SC-NEVPT2) is still contained in this subset. Hence, the maximum deviation gains more weight in the statistics, and the MUD increases for NEVPT2, while for CASPT2/CC3 the maximum deviation of 0.84 eV (2 $^1A'$ state of formamide) has been removed. This demonstrates that the statistics on which the present comparison is based are not fully saturated, and we believe that it is fair to state that CASPT2 and NEVPT2 perform similarly.

3.2.1. Excitation Energies Below 7 eV. Since Schreiber et al.[1] exclude CASPT2 and CC3 excitation energies that exceed 7 eV from the set of the best theoretical estimates, we have evaluated states below this threshold separately (Figure 2 and Table 4). It is expected that excited states above 7 eV mix with Rydberg states to a greater extend, requiring diffuse basis functions for a proper description. Since diffuse type functions are missing in the TZVP basis set, these states are also more prone to errors. Table 4 shows that the statistical deviations improve for all comparisons. In the case of NEVPT2 vs CC3, somewhat fortuitous error compensations yield a MSD of −0.07 eV (PC) and −0.01 eV (SC). For the CASPT2 vs CC3 comparison, the deviation is systematic, because the MUD is 0.14 eV and the CASPT2 excitation energies are −0.13 eV lower on average. The MUD with respect to all singlet states or the subset of CC3 single excitation weights above 90% improves slightly for NEVPT2, but more so for CASPT2. Again, this can be attributed to the maximum error, which becomes smaller for the CASPT2 comparison but remains in the subset for NEVPT2. The standard deviation in this subset is slightly higher for NEVPT2 (0.32 eV for PC and 0.29 eV for SC) than for CASPT2 (0.18 eV) in comparison to CC3. The wider spreading of NEVPT2 energies with respect to CC3 is also graphically summarized in the histograms of Figure 2. It is shown that distant deviations are excluded in the subset of singlet excitations below 7 eV in the CASPT2/CC3 distribution. This distribution is also higher peaked and more symmetric than the left-skewed NEVPT2/CC3 distribution,

Table 4. Statistical Analysis of the Singlet Excitation Energies below 7 eV with Respect to the CC3 Results

	PC-NEVPT2	SC-NEVPT2	CASPT2
count	72	72	72
MSD	−0.07 eV	−0.01 eV	−0.13 eV
MUD	0.25 eV	0.23 eV	0.14 eV
SD	0.32 eV	0.29 eV	0.18 eV
max.	−0.90 eV	−0.77 eV	−0.39 eV

dx.doi.org/10.1021/ct400136y | J. Chem. Theory Comput. XXXX, XXX, XXX−XXX

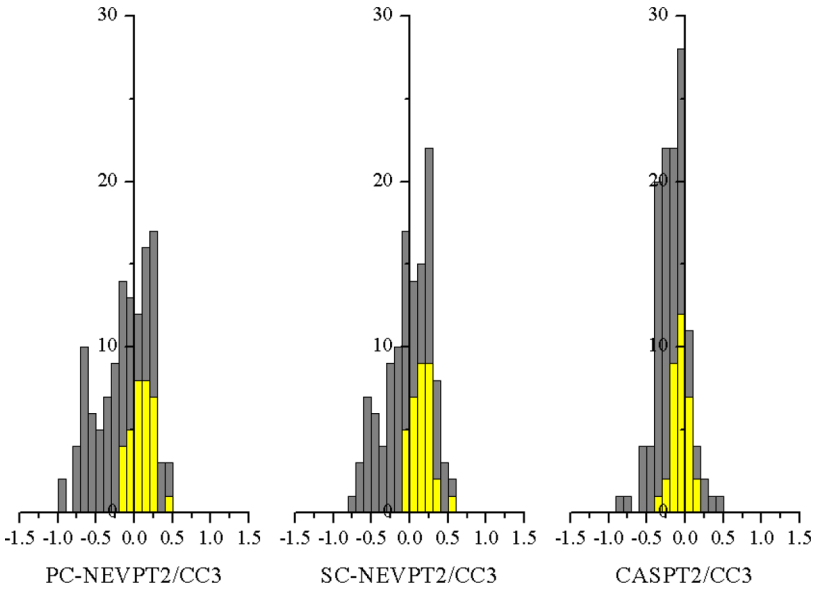

Figure 3. Histogram of the frequency of deviations in the $n \rightarrow \pi^*$ type singlet excitation energies in eV. Statistics of all excitation energies are shown in gray and $n \rightarrow \pi^*$ states are represented by yellow bars.

which shows a shoulder around −0.5 eV. This shoulder has approximately 15 excitation energies, which are responsible for less of the improvement compared to all singlet excitations. In the following, we break down the analysis by the type of excitation in order to better understand which excited states the shoulder is composed of.

3.2.2. $n \rightarrow \pi^*$ Excitations. For further analysis, it is useful to evaluate the vertical excitation energies by each excitation type separately to understand the differences between NEVPT2 and CASPT2. The excitations can be divided in the following categories: (i) $\pi \rightarrow \pi^*$ type (104 states), (ii) $n \rightarrow \pi^*$ type (45 states), and (iii) $\sigma \rightarrow \pi^*$ type (3 states). Hence, the latter type is not sufficiently well represented in this benchmark set to serve as a basis for the comparison. Visualization of the $n \rightarrow \pi^*$ state deviations in Figure 3 shows the normal distributions for NEVPT2/CC3 and CASPT2/CC3 are less distorted toward negative values. It should also be noted that the shoulder around −0.5 eV in the NEVPT2/CC3 histogram disappears, and hence, it is assigned to $\pi \rightarrow \pi^*$ excitations. The statistics improve accordingly, and a trend can be observed: NEVPT2 exaggerates the energy of $n \rightarrow \pi^*$ excitations by 0.10 eV (PC) and 0.15 eV (SC), while CASPT2 underestimates them by −0.07 eV, on average (Table 5). The mean unsigned and the standard deviations are very close to the MSD pointing to a systematic tendency, in line with the findings in Figure 3.

3.2.3. $\pi \rightarrow \pi^*$ Excitations. It follows from the results in section 3.2.2 that the asymmetry of the singlet states deviations must be mainly due to differences in the descriptions of the $\pi \rightarrow \pi^*$ transitions. Table 6 shows the statistical evaluation for this type of excitations. The SC-NEVPT2 results are closer to CC3 with a MSD of −0.08 eV as compared to −0.21 eV for PC-NEVPT2 and to −0.22 eV for CASPT2. The MUD deteriorates significantly for SC-NEVPT2, indicating a fortuitous error cancelation in MSD. However, the standard deviation is marginally larger for NEVPT2/CC3 (0.35 eV PC and 0.31 eV for SC) than for CASPT2/CC3 (0.30 eV). In contrast to $n \rightarrow \pi^*$ excitation energies, both multireference perturbation methods feature a systematic underestimation of the $\pi \rightarrow \pi^*$ state energies. Interestingly, the deviation from CC3 is the largest for this subset and at the same time NEVPT2 and CASPT2 are closer to each other than the individual comparison of either method with CC3. This can be rationalized by considering the more delocalized nature of the states involved in the $\pi \rightarrow \pi^*$ transitions, which have a multiconfigurational character that is better accounted for by the two multireference perturbation methods.

To understand the origin of the largest difference for $\pi \rightarrow \pi^*$ type of states at the NEVPT2 level, we have analyzed cases with large deviations, such as the 1^1B_u state of all-*E*-octatetraene (−0.90 eV for PC-NEVPT2/CC3 and −0.77 eV for SC-NEVPT2/CC3). The ionic nature of this state makes an accurate description a challenge for any theoretical method, because the σ-polarization[15c,17,25] and the contraction of the p-orbitals[15c,d] have to be taken into account. However, recently, Angeli et al.[15c] have investigated the 1^1B_u state of all-*E*-octatetraene where the influence of the basis set, geometry, active space size, and the order of perturbation was systematically studied. They found the augmentation of the active space with additional π^* orbitals to have an effect of 0.7 eV on the

Table 5. Statistical Analysis of the $n \rightarrow \pi^*$ Singlet Excitation Energies with Respect to the CC3 Results

	PC-NEVPT2	SC-NEVPT2	CASPT2
count	33	33	33
MSD	0.10 eV	0.15 eV	−0.07 eV
MUD	0.14 eV	0.16 eV	0.10 eV
SD	0.14 eV	0.13 eV	0.12 eV
max.	0.44 eV	0.51 eV	−0.31 eV

Table 6. Statistical Analysis of the $\pi \rightarrow \pi^*$ Singlet Excitation Energies with Respect to the CC3 Results

	PC-NEVPT2	SC-NEVPT2	CASPT2
count	85	85	85
MSD	−0.21 eV	−0.08 eV	−0.22 eV
MUD	0.33 eV	0.26 eV	0.25 eV
SD	0.35 eV	0.31 eV	0.30 eV
max.	−0.92 eV	−0.77 eV	−0.84 eV

dx.doi.org/10.1021/ct400136y | J. Chem. Theory Comput. XXXX, XXX, XXX−XXX

vertical excitation energy. The authors interpreted this as an indication for a poor zeroth-order description of the wave function, which results in an overestimation of dynamic electron correlation. This appears to be a general feature of the NEVPT2 treatment for excited states with ionic character in linear all-*trans* polyenes. Hence, it also explains the deviation found for the 1^1B_u state in all-*E*-hexatriene. The PC-NEVPT2 energy differs by −0.62 eV and SC-NEVPT2 by −0.74 eV from CC3. Expanding the number of orbitals in the active space has also shown to improve the NEVPT2 energies in this case.[26] Therefore, we assign the broad distribution of the singlet $\pi \rightarrow \pi^*$ states to the ionic states among them. These states are responsible for the underestimation of excitation energies while for the other states NEVPT2 results are typically higher in energy. This discussion is in line with earlier findings by Angeli and co-workers[15c,e] where a sensitivity of NEVPT2 energy due to the quality of the zeroth-order wave function was shown.

3.3. Triplet Excited States. The statistical evaluation of the triplet excitation energies is reported in Table 7. As already observed for the CASPT2/CC3 comparison by Schreiber et al.[1] the agreement between the investigated theoretical approaches is better for triplet excitation energies compared to singlet states, which is also reflected by the narrow distribution in the histograms of Figure 5. This is rationalized by a single excitation weight that is mostly larger than 95% in CC3. Therefore, CASPT2 and CC3 deviate by a MUD of 0.09 eV only. For NEVPT2, the mean unsigned deviation compared to CC3 is 0.16 eV (PC) and 0.17 eV (SC). It should be noticed that CASPT2 is typically underestimating the excitation energies with respect to CC3 implied by the −0.03 eV MSD while NEVPT2 rather overestimates these by 0.02 and 0.05 eV for PC and SC, respectively (Figures 4 and 5). The largest deviation between the three methods is found for the $2\ ^3B_{2u}$ state of *s*-tetrazine. The excitation energies are 6.40 eV at the PC-NEVPT2, 6.54 eV at the SC-NEVPT2, 6.83 eV at the CASPT2 and 7.36 eV at the CC3 level of theory. This state has the highest excitation energy among all investigated *s*-tetrazine triplet states and the large deviation might be due to Rydberg-valence mixing. However, this is unlikely, because of the higher singles weight of CC3. Since the transition is the only one of the $\pi \rightarrow \pi^*$ type among the higher triplet states, the large deviation is rather ascribed to the insufficient description of the zeroth-order wave function. Angeli et al.[15e] have shown a significant improvement in the description of the singlet $\pi \rightarrow \pi^*$ states of *s*-tetrazine by augmenting the active space with additional virtual π^*-type orbitals.

Table 7. Statistical Analysis of the Triplet Excitation Energies with Respect to the CC3 Results

	PC-NEVPT2	SC-NEVPT2	CASPT2
count	71	71	71
MSD	0.02 eV	0.05 eV	−0.03 eV
MUD	0.16 eV	0.17 eV	0.09 eV
SD	0.24 eV	0.22 eV	0.15 eV
max.	0.96 eV	−0.82 eV	−0.72 eV

3.4. Effect of the NEVPT2 Contraction Scheme. In this section, we compare the effect of the contraction scheme on the NEVPT2 excitation energies. The results of PC- and SC-NEVPT2 calculations are summarized in Table 1 for singlet and in Table 2 for triplet states. We find for both types of vertical excitations the difference in the relevant statistical parameters such as MUD and the standard deviation to be within 0.05 eV. For singlet states, the largest deviation between PC-NEVPT2 and SC-NEVPT2 is −0.37 eV for the $2\ ^1B_{1u}$ state of *s*-tetrazine, while for triplet states its −0.15 eV for the $2\ ^3B_{2u}$ state of *s*-tetrazine. Interestingly these states were also highlighted in the discussion above for their large deviations compared to CC3. Both states are of the $\pi \rightarrow \pi^*$ type and have strong charge transfer character. Further inspection of the singlet states in Table 3 shows that PC-NEVPT2 has a higher deviation from CC3 than SC-NEVPT2. The MUD is increasing from 0.23 to 0.28 eV and the standard deviation rises from 0.29 to 0.33 eV. This is surprising since PC-NEVPT2 is formally more accurate than SC-NEVPT2 because of the increased flexibility of the FOIS. In the case of the triplet states a small improvement of 0.01 eV in MUD is noticed in favor of PC-NEVPT2, while the standard deviation is worsened from 0.22 eV (SC-NEVPT2) to 0.24 eV (PC-NEVPT2). It should also be noted that excitation energies at the PC-NEVPT2 level are systematically lower than those at SC-NEVPT2, except for the $^1A''$ state of propanamide and two other triplet states. In summary, we find that, for all intents and purposes, the effect of the contraction scheme is found to be negligible. Such a little difference between PC- and SC-NEVPT2 is in line with numerous studies of organic compounds already documented in the literature and confirms the soundness of the strong contraction scheme.[15]

3.5. Effect of the Orbital Canonicalization Scheme. The type of the orbital canonicalization in the inactive and virtual space is expected to have an effect on the NEVPT2

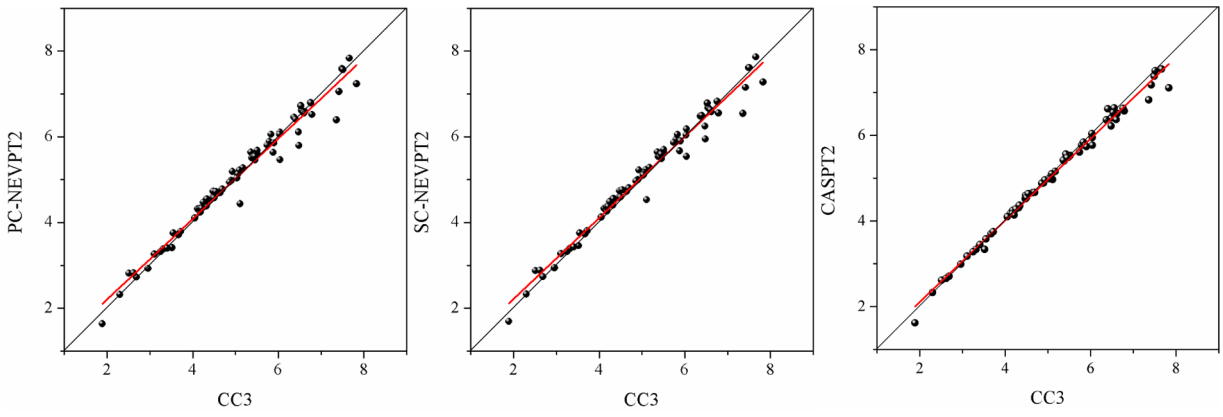

Figure 4. Correlation plots for all calculated triplet excited states. The energy is given in eV.

dx.doi.org/10.1021/ct400136y | J. Chem. Theory Comput. XXXX, XXX, XXX−XXX

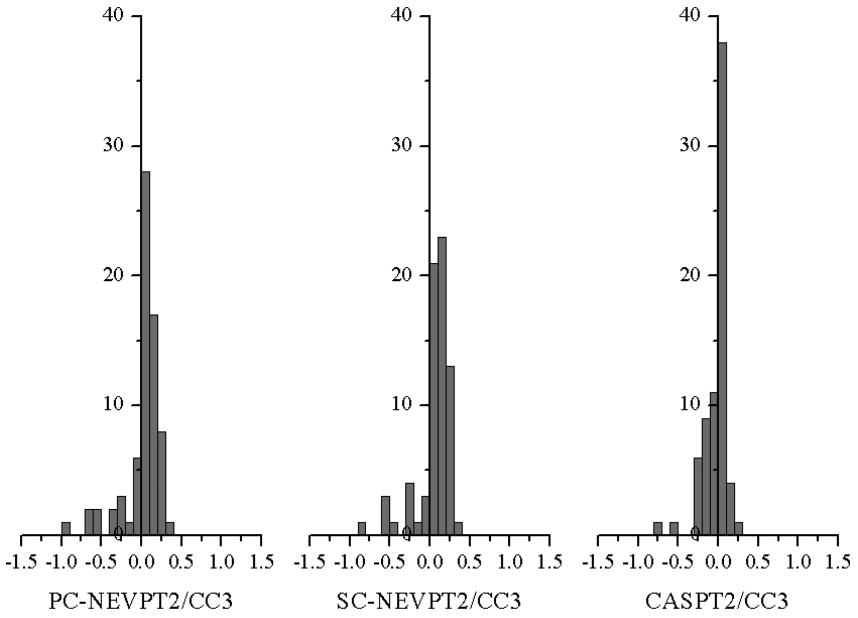

Figure 5. Histogram of the frequency of deviations in the triplet excitation energies in eV.

excitation energy. As already explained in section 2, Computational Details, there are two schemes: (i) an accurate one where the orbitals and the orbital energies are obtained from the diagonalization of the state-specific Fock operator (denoted by PC/1 and SC/1-NEVPT2) and (ii) an approximate one (denoted by PC/0 and SC/0-NEVPT2), where orbital energies are chosen as diagonal elements of the state-specific Fock operator while the orbitals remain state-averaged and pseudocanonicalized. In order to estimate the effect of this approximation, we have performed calculations for both canonicalizations. The results are summarized in Table 1 for singlet states and in Table 2 for triplet states. We find for both, the singlet and the triplet vertical excited state energies, the difference in all statistical parameters (Tables 8 and 9) to be not

Table 8. Statistical Analysis of the Singlet Excitation Energies with Respect to the CC3 Results[a]

	PC/0-NEVPT2	SC/0-NEVPT2
MSD	−0.12 eV	−0.01 eV
MUD	0.28 eV	0.24 eV
SD	0.34 eV	0.30 eV
max.	0.93 eV	0.76 eV

[a]NEVPT2 results are from the approximated orbital canonicalization scheme.

Table 9. Statistical Analysis of the Triplet Excitation Energies with Respect to the CC3 Results[a]

	PC/0-NEVPT2	SC/0-NEVPT2
MSD	0.01 eV	0.05
MUD	0.16 eV	0.17 eV
SD	0.24 eV	0.21 eV
max.	0.93 eV	0.78 eV

[a]NEVPT2 results are from the approximated orbital canonicalization scheme.

larger than one hundredth of an eV. The largest deviations between NEVPT2 excitation energies (PC and SC) using different canonicalization schemes are found to be 0.13 eV for the second $^1A_1$ excited state of formaldehyde and 0.08 eV for the ^3A_u excited state in *s*-tetrazine. In summary, the effect of the orbital canonicalization scheme is found to be negligible for the molecular systems in this benchmark set.

3.6. Effect of the IPEA Shift. Finally, we have also investigated the effect of the IPEA-shift on the CASPT2 excitation energies. Therefore we have set the IPEA shift to 0 a.u. to obtain the zeroth-order Hamiltonian in its original formulation. The results are compared to CC3 and summarized for singlet and triplet excitations in Table 10. It can be seen that

Table 10. Statistical Analysis of the CASPT2/IPEA0 Excitation Energies with Respect to the CC3 Excitation Energies for All Singlet and Triplet Excited States

	singlet	triplet
MSD	−0.48 eV	−0.37 eV
MUD	0.55 eV	0.38 eV
SD	0.62 eV	0.45 eV
max.	1.60 eV	1.50 eV

all statistical parameters change for the worse. The standard deviation for singlet excitations increases from 0.26 to 0.62 eV and for triplets from 0.15 to 0.45 eV. Especially the deviation for the triplet excitations which showed the smallest deviation with respect to CC3 has increased. The MSD is increasing from −0.03 eV to −0.37 eV while the MUD is increasing from 0.09 to 0.38 eV. The close agreement between the MSD and MUD for CASPT2/IPEA0 indicates that these energies are systematically underestimating the CC3 excitation energies. Thus, we confirm that the default IPEA shift of 0.25 a.u. strongly improves the results of this benchmark for organic compounds. However, a large benchmark of transition metal compounds and open shell systems is still missing in order to probe the general validity of the standard IPEA shift.

3.7. Further Investigation of the Reference Energies. The assessment of NEVPT2 for the calculation of excitation energies is based on comparison with CC3 reference energies. In a recent work by Noojien and co-workers,[5] a subset of this benchmark was probed by equation-of-motion (EOM)

dx.doi.org/10.1021/ct400136y | J. Chem. Theory Comput. XXXX, XXX, XXX−XXX

CCSDT-3 approach, which is closely related to CC3. Results were provided for a subset of 100 singlet states from the original Schreiber benchmark set. Although both CC3 and EOM-CCSDT-3 are considered to be close approximations to EOM-CCSDT, Noojien and co-workers have found deviations on the order of 0.1 eV between the two methods in a significant number of cases. From the theoretical point of view, EOM-CCSDT-3 is closer to EOM-CCSDT, but its accuracy with respect to Full CI has not been fully assessed. Therefore, there is no firm conclusion on the question whether CC3 or EOM-CCSDT-3 provides more accurate excitation energies. However, the authors find that EOM-CCSDT-3 values are always above CC3. Since NEVPT2 is found to overestimate the CC3 energies systematically, while CASPT2 is underestimating them, it can be expected that the choice of EOM-CCSDT-3 as a reference will change the statistics in favor of NEVPT2. Therefore, we have evaluated the subset of 100 singlet excitation energies at the EOM-CCSDT-3 level in Table 11

Table 11. Statistical Analysis for a Subset of 100 Singlet Excited States with Respect to the EOM-CCSDT-3 Results from Ref 5

	PC-NEVPT2	SC-NEVPT2	CASPT2
MSD	−0.16 eV	−0.06 eV	−0.27 eV
MUD	0.29 eV	0.23 eV	0.28 eV
SD	0.33 eV	0.29 eV	0.21 eV
max.	0.93 eV	0.74 eV	1.07 eV

and provided the analysis with respect to CC3 on the same basis in Table 12. The smallest MSD value in the comparison

Table 12. Statistical Analysis for a Subset of 100 Singlet Excited States with Respect to the CC3 Results

	PC-NEVPT2	SC-NEVPT2	CASPT2
MSD	−0.09	0.02 eV	−0.19
MUD	0.25	0.21 eV	0.21 eV
SD	0.31	0.27 eV	0.19 eV
max.	0.74	0.66 eV	0.83 eV

to EOM-CCSDT-3 is found to be −0.06 eV for SC-NEVPT2, which can be attributed to error cancelation because the MUD value is significantly larger (0.23 eV). The partially contracted variant of NEVPT2 performs slightly worse, it has a MSD of −0.16 eV and a MUD of 0.29 eV. However, in case of CASPT2, the MSD (−0.27 eV) and MUD (0.28 eV) parameters almost coincide, pointing to a systematic underestimation of excitation energies. The lower MUD value clearly indicates that NEVPT2 excitation energies are improving in comparison to CASPT2 using EOM-CCSDT-3 as a reference. However, the standard deviation is lower for CASPT2, meaning that the values are less spread. The same set of excitations at the CC3 level makes CASPT2 look marginally better for all statistical parameters (Table 11). The difference between the methods is on the order of only few hundredths eV. This change of the reference emphasizes that even a small deviation of the reference can lead to slightly different conclusions. *Cum grano salis*, we believe that the results of our benchmark calculations establish that CASPT2 and NEVPT2 are of comparable quality.

4. CONCLUSIONS

We have carried out NEVPT2 calculations of vertical excitation energies for 28 molecules in order to assess its performance for both the partially and the strongly contracted variant. In total, 225 valence excited states from the benchmark set of Schreiber et al.[1] were calculated. The same zeroth-order wave function for the multireference perturbation methods provides the basis for direct comparison of NEVPT2 and CASPT2. The detailed statistical evaluation of this data with respect to the previously published CC3 results demonstrates that for excited states of closed-shell organic molecules both methods, in their default forms, provide results of very similar accuracy and mainly differ in their details. NEVPT2 has a slightly better mean signed deviation than CASPT2, which, however, is due to cancelation of errors as shown by the unsigned and standard deviations as well as the histograms compiled in the results section.

Analyzing the limited differences between CASPT2 and NEVPT2 shows that for singlet excited states PC-NEVPT2 and SC-NEVPT2 have a standard deviation (vs CC3) of 0.33 and 0.29 eV, respectively, while CASPT2 (vs CC3) deviates by 0.26 eV. These results improve slightly upon restricting the comparison to excitations below 7 eV. Separate statistical evaluation of $\pi \rightarrow \pi^*$ and $n \rightarrow \pi^*$ transitions for singlet states and an analysis of all triplet states is carried out to rationalize the source of the deviation. The singlet excitations and, specifically, those of the $\pi \rightarrow \pi^*$ type are found to have the largest deviations among all methods. The "ionic" or "charge-transfer" nature of some of these $\pi \rightarrow \pi^*$ states is responsible for this deviation, which is the largest for all the subsets in this study. Significant improvements in the description of these states at the NEVPT2 level can be realized by improving the description of the zeroth-order wave function, for example, by additional π^* orbitals in the active space. As already pointed out by Angeli and co-workers, NEVPT2 is sensitive to the quality of the zeroth-order wave function. However, so should be any other second-order perturbation treatment of electron correlation. From the data available in the literature,[15c,27] it appears that, in this specific case, CASPT2 is not sensitive to the quality of the zeroth-order wave function. This behavior can be explained by the structure of the zeroth-order Hamiltonian, which is the Dyall Hamiltonian in case of NEVPT2. In this Hamiltonian the active orbitals include two particle terms, while the inactive and virtual orbitals consider only one-particle terms. This drastic difference in the description of different orbital spaces leads to higher sensitivity with respect to the choice of the active space. In contrast, in CASPT2's zeroth-order Hamiltonian all orbitals have a one-particle nature.[8,28] For the $n \rightarrow \pi^*$ vertical excited states PC-, SC-NEVPT2, and CASPT2 agree with CC3 up to 0.14 eV, 0.16 and 0.10 eV MSD, respectively. Moreover, for $n \rightarrow \pi^*$ transitions, the PC-NEVPT2 as well as SC-NEVPT2 exceed (0.10 and 0.15 eV MUD) while CASPT2 falls below (−0.07 eV MUD) the CC3 excitation energies.

In case of the triplet excited states, it is demonstrated that both NEVPT2 and CASPT2 agree well with CC3. On average, the signed deviation is 0.16 and 0.17 eV for PC- and SC-NEVPT2, respectively. The corresponding deviation is 0.09 eV for CASPT2 with respect to CC3. However, it is more important to note the trends: while NEVPT2 is overestimating the vertical excitations, CASPT2 is underestimating them by −0.03 eV.

dx.doi.org/10.1021/ct400136y | J. Chem. Theory Comput. XXXX, XXX, XXX−XXX

Other aspects of the benchmark were to evaluate the effect of the contraction scheme and the orbital canonicalization on the NEVPT2 excitation energies. We find that partially and strongly contracted variants perform almost equally, with former being systematically lower. However, the difference between the two contraction schemes is only few hundredths eV. Surprisingly, SC-NEVPT2 is found to be in a better agreement with CC3, although it is formally less accurate than PC-NEVPT2. In the assessment of the accurate orbital canonicalization scheme versus a more approximate one, the effect on the excitation energy is found to be below one hundredth of an eV. It demonstrates that orbital energies obtained from diagonal elements of the state-specific Fock operator and state-averaged, pseudocanonicalized orbitals are a good approximation for the type of molecules in this benchmark set.

We conclude that NEVPT2 has an overall mean unsigned deviation of 0.24 eV for the PC and 0.21 for the SC scheme with respect to CC3. CASPT2 performs slightly better (0.17 eV MUD) using the standard IPEA shift. This shift considerably improves the CASPT2 results for the molecules set in this study. However, the comparison of NEVPT2 and CASPT2 on the basis of CC3 should not be considered definite, as we demonstrate by employing EOM-CCSDT-3 data set from Nooijen and co-workers.[5] Furthermore, it should be noted that the excited states in this benchmark set were calculated for closed shell organic compounds only. An extension to address this shortcoming by including open-shell systems, a larger number of double excited, states as well as Rydberg states is desirable to obtain conclusions with a much larger range of validity. Some of these critical tests have been reported already,[8,29] but they need to be extended for systematic and statistically relevant evaluations. Furthermore, the comparison of MS-CASPT2 with QD-NEVPT2 would provide an interesting extension of this work.

AUTHOR INFORMATION

Corresponding Author

*E-mail: Frank.Neese@cec.mpg.de.

Notes

The authors declare no competing financial interest.

ACKNOWLEDGMENTS

We thank Prof. Marcel Nooijen (University of Waterloo, Canada) for stimulating discussions.

ABBREVIATIONS

NEVPT2, second order n-electron valence state perturbation theory; CASSCF, complete active space self-consistent field

REFERENCES

(1) Schreiber, M.; Silva-Junior, M. R.; Sauer, S. P.; Thiel, W. Benchmarks for electronically excited states: CASPT2, CC2, CCSD, and CC3. *J. Chem. Phys.* **2008**, *128*, 134110.

(2) Andersson, K.; Malmqvist, P.-A.; Roos, B. O. Second-order perturbation theory with a complete active space self-consistent field reference function. *J. Chem. Phys.* **1992**, *96*, 1218−1226.

(3) (a) Gadaczek, I.; Krause, K.; Hintze, K. J.; Bredow, T. MSINDO-sCIS: A new method for the calculation of excited states of large molecules. *J. Chem. Theory Comput.* **2011**, *7*, 3675−3685. (b) Trani, F.; Scalmani, G.; Zheng, G.; Carnimeo, I.; Frisch, M. J.; Barone, V. Time-dependent density functional tight binding: New formulation and benchmark of excited states. *J. Chem. Theory Comput.* **2011**, *7*, 3304−3313.

(4) (a) Peverati, R.; Truhlar, D. G. Performance of the M11 and M11-L density functionals for calculations of electronic excitation energies by adiabatic time-dependent density functional theory. *Phys. Chem. Chem. Phys.* **2012**, *14*, 11363−11370. (b) Huix-Rotllant, M.; Ipatov, A.; Rubio, A.; Casida, M. E. Assessment of dressed time-dependent density-functional theory for the low-lying valence states of 28 organic chromophores. *Chem. Phys.* **2011**, *391*, 120−129. (c) Jacquemin, D.; Perpete, E. A.; Ciofini, I.; Adamo, C. Assessment of the omega B97 family for excited-state calculations. *Theor. Chem. Acc.* **2011**, *128*, 127−136. (d) Jacquemin, D.; Perpete, E. A.; Ciofini, I.; Adamo, C.; Valero, R.; Zhao, Y.; Truhlar, D. G. On the performances of the M06 family of density functionals for electronic excitation energies. *J. Chem. Theory Comput.* **2010**, *6*, 2071−2085. (e) Silva-Junior, M. R.; Schreiber, M.; Sauer, S. P.; Thiel, W. Benchmarks for electronically excited states: Time-dependent density functional theory and density functional theory based multireference configuration interaction. *J. Chem. Phys.* **2008**, *129*, 104103.

(5) Demel, O.; Datta, D.; Nooijen, M. Additional global internal contraction in variations of multireference equation of motion coupled cluster theory. *J. Chem. Phys.* **2013**, *138*, 134108−23.

(6) (a) Angeli, C.; Cimiraglia, R.; Evangelisti, S.; Leininger, T.; Malrieu, J. P. Introduction of n-electron valence states for multi-reference perturbation theory. *J. Chem. Phys.* **2001**, *114*, 10252. (b) Angeli, C.; Cimiraglia, R.; Malrieu, J. P. n-Electron valence state perturbation theory: A fast implementation of the strongly contracted variant. *Chem. Phys. Lett.* **2001**, *350*, 297−305. (c) Angeli, C.; Cimiraglia, R. Multireference perturbation configuration interaction V. Third-order energy contributions in the Møller−Plesset and Epstein−Nesbet partitions. *Theor. Chem. Acc.* **2002**, *107*, 313−317. (d) Angeli, C.; Cimiraglia, R.; Malrieu, J. P. n-Electron valence state perturbation theory: A spinless formulation and an efficient implementation of the strongly contracted and of the partially contracted variants. *J. Chem. Phys.* **2002**, *117*, 9138−9153.

(7) Dyall, K. G. The choice of a zeroth-order Hamiltonian for second-order perturbation theory with a complete active space self-consistent-field reference function. *J. Chem. Phys.* **1995**, *102*, 4909−4918.

(8) Havenith, R. W. A.; Taylor, P. R.; Angeli, C.; Cimiraglia, R.; Ruud, K. Calibration of the n-electron valence state perturbation theory approach. *J. Chem. Phys.* **2004**, *120*, 4619−4625.

(9) Soto, J.; Avila, F. J.; Otero, J. C.; Arenas, J. F. Comment on "Multiconfigurational perturbation theory can predict a false ground state" by C. Camacho, R. Cimiraglia, and H. A. Witek. *Phys. Chem. Chem. Phys.* **2010**, *12*, 5058; *Phys. Chem. Chem. Phys.* **2011**, *13*, 7230−7231.

(10) (a) Forsberg, N.; Malmqvist, P.-Å. Multiconfiguration perturbation theory with imaginary level shift. *Chem. Phys. Lett.* **1997**, *274*, 196−204. (b) Roos, B. O.; Andersson, K. Multiconfigurational perturbation theory with level shift the Cr_2 potential revisited. *Chem. Phys. Lett.* **1995**, *245*, 215−223. (c) Witek, H. A.; Choe, Y.-K.; Finley, J. P.; Hirao, K. Intruder state avoidance multireference Møller−Plesset perturbation theory. *J. Comput. Chem.* **2002**, *23*, 957−965.

(11) Ghigo, G.; Roos, B. O.; Malmqvist, P.-Å. A modified definition of the zeroth-order Hamiltonian in multiconfigurational perturbation theory (CASPT2). *Chem. Phys. Lett.* **2004**, *396*, 142−149.

(12) (a) Karlström, G.; Lindh, R.; Malmqvist, P.-Å.; Roos, B. O.; Ryde, U.; Veryazov, V.; Widmark, P.-O.; Cossi, M.; Schimmelpfennig, B.; Neogrady, P.; Seijo, L. MOLCAS: A program package for computational chemistry. *Comput. Mater. Sci.* **2003**, *28*, 222−239. (b) Andersson, K.; Aquilante, F.; Barysz, M.; Bednarz, E.; Bernhardsson, A.; Blomberg, M. R. A.; Carissan, Y.; Cooper, D. L.; Cossi, M.; Devarajan, A.; Vico, L. D.; Ferré, N.; Fülscher, M. P.; Gaenko, A.; Gagliardi, L.; Ghigo, G.; de Graaf, C.; Hess, B. A.; Hagberg, D.; Holt, A.; Karlström, G.; Krogh, J. W.; Lindh, R.; Malmqvist, P.-Å.; Nakajima, T.; Neogrády, P.; Olsen, J.; Pedersen, T. B.; Raab, J.; Reiher, M.; Roos, B. O.; Ryde, U.; Schimmelpfennig, B.; Schütz, M.; Seijo, L.; Serrano-Andrés, L.; Siegbahn, P. E. M.; Stålring, J.; Thorsteinsson, T.; Veryazov, V.; Widmark, P.-O.; Wolf, A. Molcas.

(13) (a) Lawson Daku, L. M.; Aquilante, F.; Robinson, T. W.; Hauser, A. Accurate spin-state energetics of transition metal complexes: I. CCSD(T), CASPT2, and DFT study of [M(NCH)6]2+ (M = Fe, Co). *J. Chem. Theory Comput.* **2012**, *8*, 4216−4231. (b) Kepenekian, M.; Robert, V.; Le Guennic, B. What zeroth-order Hamiltonian for CASPT2 adiabatic energetics of Fe(II)N[sub 6] architectures? *J. Chem. Phys.* **2009**, *131*, 114702−8.

(14) Angeli, C.; Pastore, M.; Cimiraglia, R. New perspectives in multireference perturbation theory: The n-electron valence state approach. *Theor. Chem. Acc.* **2007**, *117*, 743−754.

(15) (a) Valsson, O.; Angeli, C.; Filippi, C. Excitation energies of retinal chromophores: Critical role of the structural model. *Phys. Chem. Chem. Phys.* **2012**, *14*, 11015−11020. (b) Pastore, M.; Angeli, C.; Cimiraglia, R. The vertical electronic spectrum of pyrrole: A second and third order n-electron valence state perturbation theory study. *Chem. Phys. Lett.* **2006**, *422*, 522−528. (c) Angeli, C.; Pastore, M. The lowest singlet states of octatetraene revisited. *J. Chem. Phys.* **2011**, *134*, 184302. (d) Angeli, C. On the nature of the $\pi \rightarrow \pi^*$ ionic excited states: The V state of ethene as a prototype. *J. Comput. Chem.* **2009**, *30*, 1319−1333. (e) Angeli, C.; Cimiraglia, R.; Cestari, M. A multireference n-electron valence state perturbation theory—Study of the electronic spectrum of s-tetrazine. *Theor. Chem. Acc.* **2009**, *123*, 287−298.

(16) (a) Angeli, C.; Borini, S.; Cimiraglia, R. An application of second-order n-electron valence state perturbation theory to the calculation of excited states. *Theor. Chem. Acc.* **2004**, *111*, 352−357. (b) Angeli, C.; Borini, S.; Ferrighi, L.; Cimiraglia, R. Ab initio n-electron valence state perturbation theory study of the adiabatic transitions in carbonyl molecules: Formaldehyde, acetaldehyde, and acetone. *J. Chem. Phys.* **2005**, *122*, 114304.

(17) Angeli, C. An analysis of the dynamic σ polarization in the V state of ethene. *Int. J. Quantum Chem.* **2010**, *110*, 2436−2447.

(18) Pastore, M.; Angeli, C.; Cimiraglia, R. An application of second and third-order n-electron valence state perturbation theory to the calculation of the vertical electronic spectrum of furan. *Chem. Phys. Lett.* **2006**, *426*, 445−451.

(19) (a) Cronstrand, P.; Christiansen, O.; Norman, P.; Agren, H. Theoretical calculations of excited state absorption. *Phys. Chem. Chem. Phys.* **2000**, *2*, 5357−5363. (b) Christiansen, O.; Koch, H.; Jorgensen, P. Response functions in the CC3 iterative triple excitation model. *J. Chem. Phys.* **1995**, *103*, 7429−7441. (c) Hald, K.; Hattig, C.; Olsen, J.; Jorgensen, P. CC3 triplet excitation energies using an explicit spin coupled excitation space. *J. Chem. Phys.* **2001**, *115*, 3545−3552. (d) Koch, H.; Christiansen, O.; Jorgensen, P.; Olsen, J. Excitation-energies of BH, CH_2, and Ne in full configuration-interaction and the hierarchy CCS, CC2, CCSD, and CC3 of coupled-cluster models. *Chem. Phys. Lett.* **1995**, *244*, 75−82. (e) Christiansen, O.; Koch, H.; Jorgensen, P.; Olsen, J. Excitation energies of H_2O, N_2 and C_2 in full configuration interaction and coupled cluster theory. *Chem. Phys. Lett.* **1996**, *256*, 185−194. (f) Pecul, M.; Jaszunski, M.; Larsen, H.; Jorgensen, P. Singlet excited states of Be_2. *J. Chem. Phys.* **2000**, *112*, 3671−3679. (g) Larsen, H.; Olsen, J.; Jorgensen, P.; Christiansen, O. Full configuration interaction benchmarking of coupled-cluster models for the lowest singlet energy surfaces of N_2. *J. Chem. Phys.* **2000**, *113*, 6677−6686. (h) Larsen, H.; Hald, K.; Olsen, J.; Jorgensen, P. Triplet excitation energies in full configuration interaction and coupled-cluster theory. *J. Chem. Phys.* **2001**, *115*, 3015−3020. (i) Hald, K.; Jorgensen, P.; Breckenridge, W. H.; Jaszunski, M. Calculation of ground and excited state potential energy curves of the MgAr complex using the coupled cluster approximate triples model CC3. *Chem. Phys. Lett.* **2002**, *364*, 402−408.

(20) Schafer, A.; Horn, H.; Ahlrichs, R. Fully optimized contracted Gaussian basis sets for atoms Li to Kr. *J. Chem. Phys.* **1992**, *97*, 2571−2577.

(21) Neese, F. The ORCA program system. *Wiley Interdiscip. Rev.: Comput. Mol. Sci.* **2012**, *2*, 73−78.

(22) Werner, H.-J.; Knowles, P. J.; Knizia, G.; Manby, F. R.; Schütz, M.; Celani, P.; Korona, T.; Lindh, R.; Mitrushenkov, A.; Rauhut, G.; Shamasundar, K. R.; Adler, T. B.; Amos, R. D.; Bernhardsson, A.; Berning, A.; Cooper, D. L.; Deegan, M. J. O.; Dobbyn, A. J.; Eckert, F.; Goll, E.; Hampel, C.; Hesselmann, A.; Hetzer, G.; Hrenar, T.; Jansen, G.; Köppl, C.; Liu, Y.; Lloyd, A. W.; Mata, R. A.; May, A. J.; McNicholas, S. J.; Meyer, W.; Mura, M. E.; Nicklass, A.; O'Neill, D. P.; Palmieri, P.; Peng, D.; Pflüger, K.; Pitzer, R.; Reiher, M.; Shiozaki, T.; Stoll, H.; Stone, A. J.; Tarroni, R.; Thorsteinsson, T.; Wang, M. *MOLPRO*, version 2012.1, a package of ab initio programs; University College Cardiff Consultants Limited: Cardiff, 2012.

(23) Finley, J.; Malmqvist, P.-Å.; Roos, B. O.; Serrano-Andrés, L. The multi-state CASPT2 method. *Chem. Phys. Lett.* **1998**, *288*, 299−306.

(24) Angeli, C.; Borini, S.; Cestari, M.; Cimiraglia, R. A quasidegenerate formulation of the second order n-electron valence state perturbation theory approach. *J. Chem. Phys.* **2004**, *121*, 4043−4049.

(25) (a) Davidson, E. R. The spatial extent of the V state of ethylene and its relation to dynamic correlation in the cope rearrangement. *J. Phys. Chem.* **1996**, *100*, 6161−6166. (b) Boggio-Pasqua, M.; Bearpark, M. J.; Klene, M.; Robb, M. A. A computational strategy for geometry optimization of ionic and covalent excited states, applied to butadiene and hexatriene. *J. Chem. Phys.* **2004**, *120*, 7849−7860.

(26) (a) Gaureschi, R. Ab initio study of the spectroscopy of hexatriene with the NEVPT2 approach. Master Thesis, Università degli studi di Ferrara, Ferrara, Italy, 2012; (b) Gozem, S.; Huntress, M.; Schapiro, I.; Lindh, R.; Granovsky, A. A.; Angeli, C.; Olivucci, M. Dynamic electron correlation effects on the ground state potential energy surface of a retinal chromophore model. *J. Chem. Theory Comput.* **2012**, *8*, 4069−4080.

(27) Angeli, C.; Bories, B.; Cavallini, A.; Cimiraglia, R. Third-order multireference perturbation theory: The n-electron valence state perturbation-theory approach. *J. Chem. Phys.* **2006**, *124*, 054108.

(28) Roca-Sanjuán, D.; Aquilante, F.; Lindh, R. Multiconfiguration second-order perturbation theory approach to strong electron correlation in chemistry and photochemistry. *Wiley Interdiscip. Rev.: Comput. Mol. Sci.* **2012**, *2*, 585−603.

(29) Domingo, A.; Carvajal, M.; Graaf, C.; Sivalingam, K.; Neese, F.; Angeli, C. Metal-to-metal charge-transfer transitions: Reliable excitation energies from ab initio calculations. *Theor. Chem. Acc.* **2012**, *131*, 1−13.